

# Identification of a novel *FN1–FGFR1* genetic fusion as a frequent event in phosphaturic mesenchymal tumour

Jen-Chieh Lee,<sup>1</sup> Yung-Ming Jeng,<sup>1†</sup> Sheng-Yao Su,<sup>2,3†</sup> Chen-Tu Wu,<sup>1</sup> Keh-Sung Tsai,<sup>4</sup> Cheng-Han Lee,<sup>5</sup> Chung-Yen Lin,<sup>2</sup> Jodi M Carter,<sup>6</sup> Jenq-Wen Huang,<sup>4</sup> Shu-Hwa Chen,<sup>7</sup> Shyang-Rong Shih,<sup>4</sup> Adrián Mariño-Enríquez,<sup>7</sup> Chih-Chi Chen,<sup>1</sup> Andrew L Folpe,<sup>6</sup> Yih-Leong Chang<sup>1\*</sup> and Cher-Wei Liang<sup>1\*</sup>

<sup>1</sup> Department of Pathology, National Taiwan University Hospital and National Taiwan University College of Medicine, Taipei, Taiwan

<sup>2</sup> Institute of Information Science, Academia Sinica, Taipei, Taiwan

<sup>3</sup> Bioinformatics Program, Taiwan International Graduate Program, Academia Sinica & Institute of Biomedical Informatics, National Yang-Ming University, Taipei, Taiwan

<sup>4</sup> Department of Internal Medicine, National Taiwan University Hospital and National Taiwan University College of Medicine, Taipei, Taiwan

<sup>5</sup> Department of Laboratory Medicine and Pathology, University of Alberta and Royal Alexandra Hospital, Edmonton, Alberta, Canada

<sup>6</sup> Department of Laboratory Medicine and Pathology, Mayo Clinic, Rochester, MN, USA

<sup>7</sup> Department of Pathology, Brigham and Women's Hospital, Harvard Medical School, Boston, MA, USA

\*Correspondence to: Yih-Leong Chang, MD, Department of Pathology, National Taiwan University Hospital and National Taiwan University College of Medicine, 7 Chong-Shan South Road, Taipei, Taiwan 100. E-mail: ntuhylc@gmail.com

Or Cher-Wei Liang, MD, Department of Pathology, National Taiwan University Hospital and National Taiwan University College of Medicine, 7 Chong-Shan South Road, Taipei, Taiwan 100. E-mail: 018511@ntuh.gov.tw

†These authors contributed equally to this study.

## Abstract

Phosphaturic mesenchymal tumours (PMTs) are uncommon soft tissue and bone tumours that typically cause hypophosphataemia and tumour-induced osteomalacia (TIO) through secretion of phosphatonins including fibroblast growth factor 23 (FGF23). PMT has recently been accepted by the World Health Organization as a formal tumour entity. The genetic basis and oncogenic pathways underlying its tumourigenesis remain obscure. In this study, we identified a novel *FN1–FGFR1* fusion gene in three out of four PMTs by next-generation RNA sequencing. The fusion transcripts and proteins were subsequently confirmed with RT-PCR and western blotting. Fluorescence *in situ* hybridization analysis showed six cases with *FN1–FGFR1* fusion out of an additional 11 PMTs. Overall, nine out of 15 PMTs (60%) harboured this fusion. The *FN1* gene possibly provides its constitutively active promoter and the encoded protein's oligomerization domains to overexpress and facilitate the activation of the *FGFR1* kinase domain. Interestingly, unlike the prototypical leukaemia-inducing *FGFR1* fusion genes, which are ligand-independent, the *FN1–FGFR1* chimeric protein was predicted to preserve its ligand-binding domains, suggesting an advantage of the presence of its ligands (such as FGF23 secreted at high levels by the tumour) in the activation of the chimeric receptor tyrosine kinase, thus effecting an autocrine or a paracrine mechanism of tumourigenesis.

Copyright © 2014 Pathological Society of Great Britain and Ireland. Published by John Wiley & Sons, Ltd.

**Keywords:** phosphaturic mesenchymal tumour; translocation; *FN1*; *FGFR1*; RNA sequencing

Received 1 August 2014; Revised 24 September 2014; Accepted 13 October 2014

No conflicts of interest were declared.

## Introduction

Phosphaturic mesenchymal tumour (PMT) is a soft tissue or bone neoplasm that usually presents with intractable hypophosphataemia and tumour-induced osteomalacia (TIO) [1,2], often mediated by tumour secretion of fibroblast growth factor 23 (FGF23). FGF23, a phosphatonin also implicated in familial tumoural calcinosis and X-linked hypophosphataemic rickets, decreases 1,25-dihydroxyvitamin D3 production and promotes renal phosphate wasting [3].

Historically, a variety of different mesenchymal tumours were thought to cause TIO. However, recent

studies have shown that the vast majority of cases are caused by a morphologically distinctive neoplasm, ie PMT [2,4]. Pathologically, PMT is characterized by a hypervascular proliferation of bland, spindled cells associated with a variable amount of 'smudgy' calcified matrix. A small subset of PMTs exhibit malignant histological features and may behave in a clinically malignant fashion [2].

PMTs often overexpress a variety of phosphatonins, including FGF23, secreted frizzled-related protein 4 (sFRP4), and matrix extracellular phosphoglycoprotein (MEPE) [3,5]. Of these, FGF23 is the best studied.

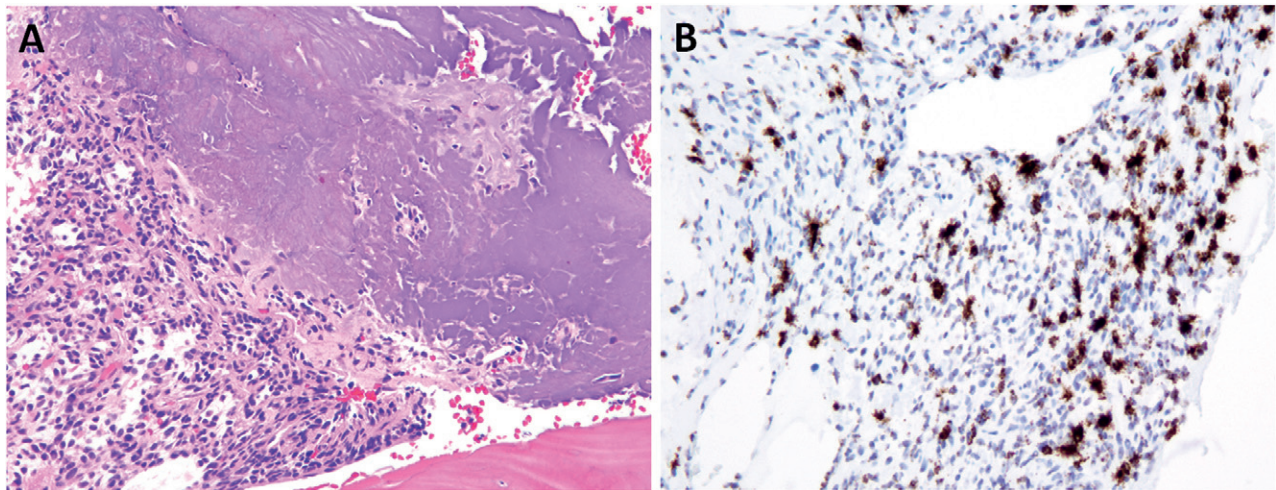


Figure 1. (A) Histology of PMT. The tumour is composed of spindle to ovoid cells, commonly admixed with a variable amount of osteoid or chondroid matrix. (B) RNAscope<sup>®</sup> CISH demonstrates *FGF23* mRNA in the tumour tissue. Original magnification:  $\times 200$ .

Physiologically, FGF23 is secreted chiefly by osteocytes and acts primarily on proximal renal tubular cells. Unlike most other FGF family members, the binding of FGF23 to FGF receptors (FGFRs) normally requires  $\alpha$ -Klotho, a transmembrane co-receptor. However, high levels of FGF23 may activate FGFRs in the absence of Klotho [6].

Genetic aberrations involving FGFRs have been linked with various neoplastic and non-neoplastic disorders [7,8]. The best-established receptor of FGF23 is FGFR1, which on ligand binding and activation conducts its signalling pathways to regulate cell proliferation, survival, migration, and differentiation [9]. *FGFR1* genetic translocations cause a group of leukaemic diseases, known collectively as '8p11 myeloproliferative syndrome', wherein the transmembrane domain of FGFR1 is fused to the N-terminus of a constitutively expressed partner protein that dimerizes or oligomerizes to initiate ligand-independent activation of FGFR1 kinase domains [10]. To date, however, the genetic mechanisms underlying the pathogenesis of PMT, including neoplastic FGF23 overexpression, remain obscure.

In this study, we have employed high-throughput next-generation sequencing of the tumour transcriptome and fluorescence *in situ* hybridization (FISH) and identified *FNI-FGFR1* fusion genes in 60% (9/15) of PMTs.

## Materials and methods

### Tumour samples

Frozen or paraffin-embedded samples were collected from the pathology archive and consultation files of the National Taiwan University Hospital (Taipei, Taiwan) and the Mayo Clinic (Rochester, MN, USA), with the diagnosis confirmed by an experienced pathologist (ALF). Representative histology is demonstrated in Figure 1A. Eleven patients had clinical TIO

and/or hypophosphataemia, and in 14 cases, tumoural expression of *FGF23* mRNA was demonstrated by RNAscope<sup>®</sup> CISH, using previously published methods (Figure 1B) [11]. This research was approved by the respective institutional ethical boards (N.T.U.H., 201211081RIC; Mayo Clinic, 10-6605). The clinical information is summarized in Table 1.

### RNA sequencing

Total RNA was extracted with Trizol Reagent (Life Technologies, Carlsbad, CA, USA), depleted of ribosomal RNA with a Ribo-Zero Gold kit (Illumina, San Diego, CA, USA), and then qualified with a Bioanalyser 2100 using an RNA 6000 labchip kit (Agilent Technologies, Santa Clara, CA, USA). RNA libraries were constructed with TruSeq RNA Sample Prep Kits for 101-bp paired-end sequencing on an Illumina HiSeq2000 platform using TruSeq SBS Kit v3-HS. UCSC human genome hg19 was used as the mapping reference. The raw data were uploaded to the NCBI SRA repository (accession SRP045126; <http://www.ncbi.nlm.nih.gov/sra/SRP045126>). Details of fusion detection and gene expression profiling may be found in Supplementary Table 1 and the Supplementary methods.

### PCR and direct sequencing

Genomic DNA and total RNA were extracted from frozen tissue and formalin-fixed, paraffin-embedded (FFPE) tumour tissue, respectively, using a QIAamp DNA Micro Kit (Qiagen, Venlo, The Netherlands) and a RecoverAll Total Nucleic Acid Isolation Kit (Life Technologies) according to the manufacturers' instructions. Polymerase chain reaction (PCR) with/without reverse transcription was performed as previously described [12]. Primers specific for *FNI* and *FGFR1* were designed to amplify the regions flanking the breakpoints of genomic DNA (including reciprocal fusions) and fusion transcripts (Supplementary Table 2).

Table 1. Summary of clinical and molecular findings

Case No	Sex	Age (years)	Location	TIO/HPS	FGF23 CISH	RNA sequencing	<i>FN1-FGFR1</i> fusion FISH*	Note
PMT-1 <sup>†</sup>	M	44	Thigh	Present	Positive	<i>FN1-FGFR1</i>	Positive (21.2%)	
PMT-2 <sup>†</sup>	F	57	Thigh	Present	Positive	<i>FN1-FGFR1</i>	Positive (21.5%)	
PMT-3	M	43	Toe	NP	Negative	<i>FN1-FGFR1</i>	Failed	
PMT-4	F	46	Back	Present	Positive	No fusion found	Negative (6.1%)	
PMT-5	M	55	Ankle	Present	Positive	NP	Positive (40.5%)	
PMT-6	M	50	Thigh	Present	Positive	NP	Positive (25.4%)	
PMT-7	M	50	Lower leg	NP	Positive	NP	Positive (22%)	
PMT-8	F	48	Femur	Present	Positive	NP	Positive (15.1%)	
PMT-9 <sup>‡</sup>	M	61	Iliopsoas	Present	Positive	NP	Positive (12.4%)	
PMT-10	M	69	Foot	NP	Positive	NP	Positive (10.7%)	Chronic renal failure
PMT-11	M	53	Thigh	NP	Positive	NP	Negative (5.3%)	
PMT-12	M	65	Pelvis	Present	Positive	NP	Negative (4.4%)	
PMT-13	F	62	Thigh	Present	Positive	NP	Negative (4.0%)	Malignant PMT
PMT-14	M	61	Buttock	Present	Positive	NP	Negative (3.6%)	
PMT-15 <sup>‡</sup>	M	47	Shoulder	Present	Positive	NP	Negative (3.3%)	

\*Numbers in parentheses indicate the percentage of nuclei that harbour fusion signals.

<sup>†</sup>These cases have frozen tumour samples.

<sup>‡</sup>These cases have been karyotyped previously, without demonstrable recurrent chromosomal abnormality [14].

CISH = chromogenic *in situ* hybridization; NP = not present/performed; TIO/HPS = tumour-induced osteomalacia and/or hypophosphataemic syndrome.

Purified PCR products were Sanger-sequenced using a BigDye v3.1 cycle sequencing kit on an ABI-3730 DNA analyser (Applied Biosystems, Foster City, CA, USA).

**Western blotting**

Protein lysates (100 µg) of frozen tumours and control cell lines were separated by 10% SDS-PAGE, electro-transferred onto nitrocellulose membranes (Amersham, Buckinghamshire, UK), and incubated with a primary antibody against FGFR1 (Cell Signaling Technology, Danvers, MA, USA) followed by a secondary antibody (goat anti-rabbit IgG; 1 : 5000 dilution; Santa Cruz Biotechnology, Santa Cruz, CA, USA). Immunoreactivity was detected using an enhanced chemiluminescence kit (Millipore, Bedford, MA, USA).

**FISH analysis**

FISH probes were synthesized by Empire Genomics, Inc (Buffalo, NY, USA), using bacterial artificial chromosomes RP11-585P16, RP11-640F19, and RP11-300D18 to cover 5' regions of the *FN1* gene and RP11-265K5, RP11-90P5, and RP11-933I10 to cover 3' of *FGFR1*. Interphase FISH was performed on 4-µm-thick FFPE tissue sections as previously described [13]. At least 50 nuclei were counted for each slide. Fusion signals were defined as two differently labelled signals that were less than half the average width of a signal apart. A tissue microarray containing 48 carcinomas of eight common types served as a negative control which helped to determine the threshold of a positive result. At least 200 nuclei were counted for cases where the percentage of nuclei with fusion signals fell within the range of threshold level ±3%.

**Results and discussion**

*FN1-FGFR1* fusion gene was detected by RNA sequencing in three out of four PMTs (Supplementary

Table 3). Two alternative fusion transcript forms were observed in PMT-1 and PMT-2 apiece. In PMT-1, *FN1* gene breakpoint at the 3' end of exon 23 was fused to the 5' ends of exon 3 and exon 4, respectively, of the *FGFR1* gene. In PMT-2, the 3' end of exon 22 of the *FN1* gene was fused to identical breakpoints of the *FGFR1* gene identified in PMT-1. Interestingly, there were minor reads spanning non-random junctions between intron 23 (PMT-1) or intron 22 (PMT-2) of *FN1* and intron 2 of *FGFR1* (Supplementary Table 3). These reads probably originated from unspliced mRNA precursors or genomic DNA contaminants and indicated 'real' breakpoints at the DNA level. In PMT-3, a different *FN1-FGFR1* fusion was found between the 3' end of exon 28 of *FN1* and the 5' end of exon 5 of *FGFR1*. All the fusions were predicted to be in-frame.

The gene expression levels are shown in Supplementary Table 4. The four PMTs highly expressed *FN1* and *FGFR1*, as well as the phosphatonin genes *FGF23*, *MEPE*, and *SFRP4*. Except *FGF1*, the remaining FGF genes were expressed at low levels, and so was the *KL* gene. These results were corroborated by the heatmap plot in comparison to the expression of respective genes in other tumour types (Supplementary Figure 1). Both the MDS and the PCA plots demonstrated, transcriptome-wise, that PMT-1 and PMT-2 clustered closely (Supplementary Figure 2). These results suggest that PMT is a distinctive entity with considerable homogeneity, although the sample size is too small to draw a definite conclusion.

All five variants of the *FN1-FGFR1* fusion transcripts as well as the DNA breakpoints in PMT-1 and PMT-2 were further verified by RT-PCR and PCR, respectively, with bidirectional Sanger sequencing (Supplementary Figure 3 and Figure 2A). Furthermore, FGFR1 immunoblotting using protein lysates from both PMT-1 and PMT-2 revealed bands at 160–170 kD and >200 kD, larger than the normal counterparts (Figure 2B). This result corroborated the expression by

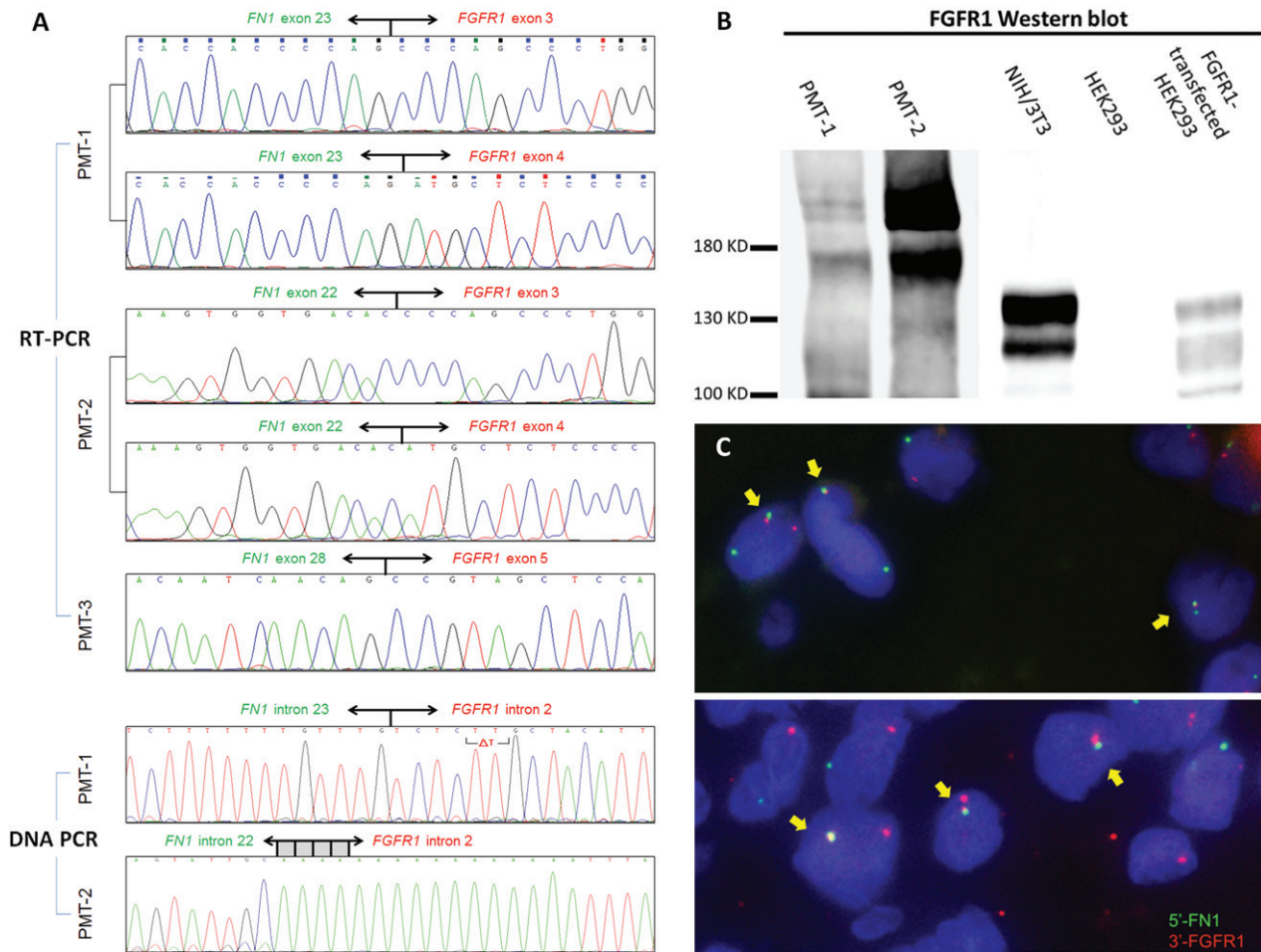


Figure 2. (A) Sanger sequencing of the RT-PCR and DNA PCR products demonstrating the different fusion points. Deletion of one thymidine ( $\Delta T$ ) was found near the intronic fusion point in PMT-1. (B) Western blot of two PMTs and control cells (composited image). Both PMT-1 and PMT-2 revealed bands at 160–170 and  $>200$  kD. NIH/3T3 cells expressed endogenous murine FGFR1 (120 and 145 kD), comparable in size to human FGFR1. HEK293 cells transfected with a full-length FGFR1 construct, showing an additional band at 100 kD, served as a control. (C) Detection of *FN1-FGFR1* fusion by FISH in PMT-2 (upper) and PMT-7 (lower). The 5'-*FN1* and 3'-*FGFR1* loci are labelled in green and orange, respectively. The fusion signals present as a pair of green and red signals in close proximity or fused into a yellow signal, as indicated by arrows.

PMTs of the in-frame chimeric FGFR1 proteins with increased molecular weights.

An expanded group of PMTs was subsequently checked for *FN1-FGFR1* fusion by FISH. Of the 15 PMTs and 48 control cases tested, 14 and 29 had interpretable results, respectively (Table 1). The 'fusion' signals were present in 0–3.9% (mean 1.69%, standard deviation 1.05%) of nuclei in the control cases. Accordingly, a cut-off threshold was defined as 10%. Using this criterion, eight PMTs were positive (range 10.7–40.5%; median 21.35%; Figure 2C).

Overall, we identified a novel *FN1-FGFR1* fusion gene in 60% (9/15) of PMTs. The predicted domains retained in the fusion protein are illustrated in Figure 3A. The high prevalence of this fusion gene strongly suggests that it plays a role in PMT tumourigenesis and supports the classification of PMT as a specific entity, although its absence in 40% of the cases suggests that genetic heterogeneity does exist. Of note, the oftentimes significant population of non-neoplastic cells in PMT might account for the relatively low percentage

of cells harbouring fusion signals, and could even lead to false-negative results. Importantly, the fusion partners (5' *FN1* and 3' *FGFR1*) are both telomeric in direction; thus, the fusion events might take unusual forms, such as insertion of a chromosomal segment containing one partner gene into the other, instead of a simple reciprocal t(2;8) translocation where the derivative chromosome harbouring the *FN1(5')-FGFR1(3')* fusion gene would lose its centromere (Supplementary Figure 4). Consistent with this theory, the presumed reciprocal fusion gene (*5'FGFR1-3'FN1*) was not found by RNA sequencing or DNA PCR (Supplementary Table 3 and Supplementary Figure 3). Such an inserting segment can be too small to be recognized by conventional karyotyping or even FISH analysis. Intriguingly, although a prior cytogenetic study showed no evidence of t(2;8) [14], we found that PMT-9 harboured infrequent fusion signals by FISH. It remains to be determined whether this represents a small insertion or intra-tumoural heterogeneity. Interestingly, PMT-4, which was negative for *FN1-FGFR1* fusion, expressed

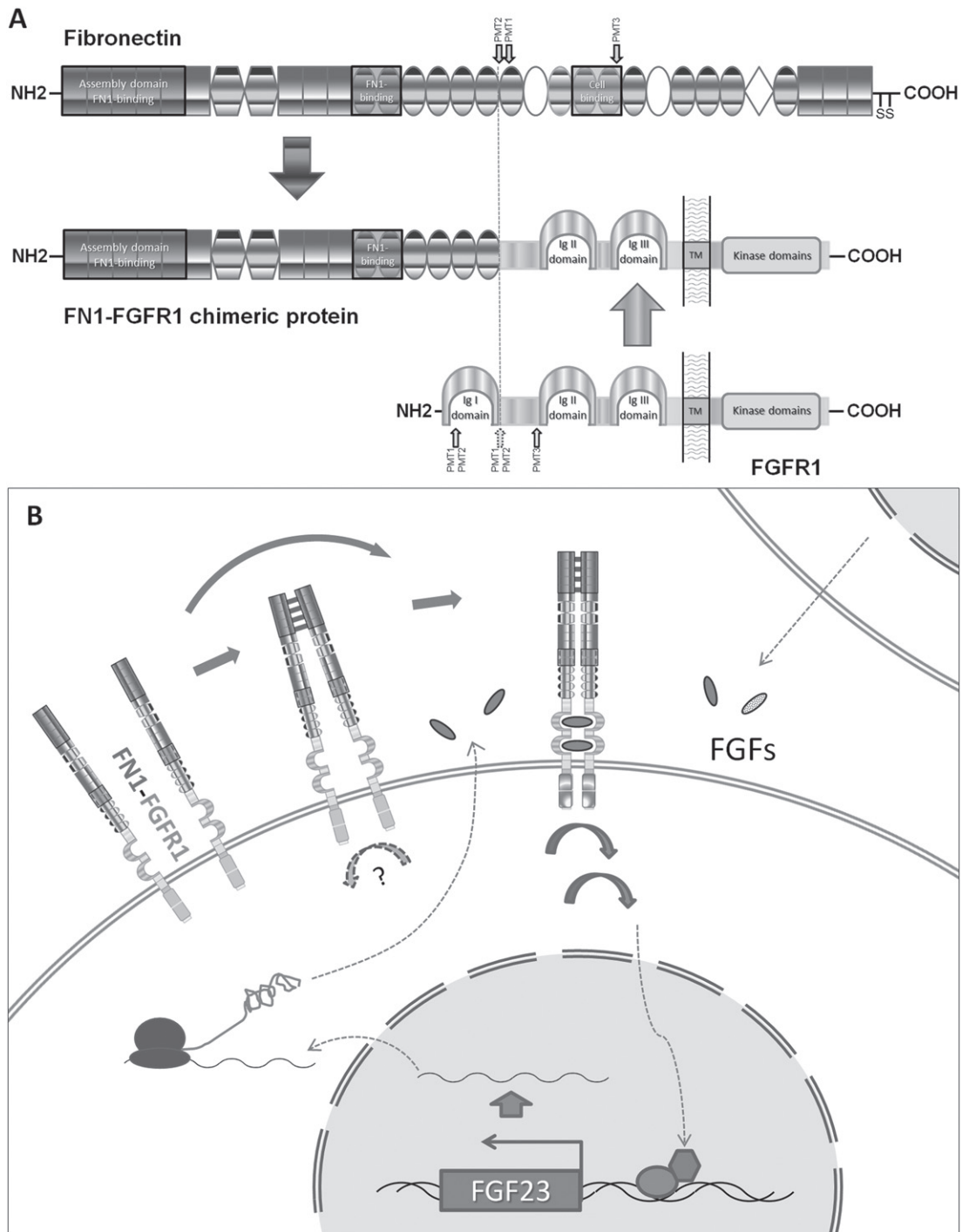


**Figure 3.** (A) Predicted domains retained in the chimeric protein. Small arrows indicate the breakpoints of various transcripts in respective tumour samples. The small dotted arrow indicates the breakpoint with the *FGFR1* exon 3 spliced out. TM indicates the transmembrane domain. Illustrated in the middle is the predominant form of fusion transcript in PMT-2. Note that the FN1-binding self-association domains of fibronectin and two of the three ligand-binding Ig-like domains of FGFR1 are predicted to be retained in all transcript variants [20]. (B) The proposed hypotheses of the autocrine/paracrine loop mechanism of PMT tumorigenesis driven by the *FN1-FGFR1* fusion gene. The fusion receptor may possibly dimerize through fibronectin self-association and/or FGF ligand binding and activate the kinase domains to conduct the FGFR1 signalling pathways, whereby FGF23 may be up-regulated and in turn promote the activation of FN1-FGFR1. Other FGFs (such as FGF1) may also play a role.

a high level of FGFR1 and had an expression profile similar to those of the other PMTs, suggesting an alternative fusion partner or mechanism that up-regulates FGFR1 and its downstream signalling pathways.

The high consistency of the *FN1* gene as a fusion partner implies important functional roles. *FN1* encodes

fibronectin, an extracellular matrix component constitutively expressed by many cell types. In PMT, *FN1* probably provides its promoter to overexpress the 3' *FGFR1*. Furthermore, fibronectin can polymerize to form superfibronectin, which may put multiple C'-FGFR1 molecules in physical proximity, facilitating

their transphosphorylation and activation. Interestingly, a novel *FN1-ALK* fusion gene with demonstrable transforming ability has been recently identified in an ovarian stromal sarcoma, with an *FN1* breakpoint identical to that identified in PMT-1 [15]. It is reasonable to speculate that the same mechanisms whereby *FN1-ALK* is activated might also apply to *FN1-FGFR1*.

As a well-known oncogene, *FGFR1* has been implicated in a variety of human cancers through amplification, translocations, and mutations [8]. Remarkably, unlike the prototypical *FGFR1* fusion proteins in the 8p11 myeloproliferative syndrome, the PMT-associated *FN1-FGFR1* fusion protein is predicted to retain at least two of three extracellular FGF-binding (Ig-like) domains. As PMT secretes FGF23, an *FGFR1* ligand, FGF binding possibly contributes to PMT tumorigenesis through an autocrine or a paracrine signalling paradigm. Interestingly, all four PMTs subjected to RNA sequencing showed minimal expression of  $\alpha$ -Klotho, a usually obligatory co-receptor for FGF23-*FGFR1* binding. Perhaps frequent loss of the first Ig-like domain (through genetic fusion or alternative splicing; Figure 3A) in the *FN1-FGFR1* fusion protein might enhance its binding affinity to FGF23, as previously shown [16], and render the presence of  $\alpha$ -Klotho non-obligatory, especially in a microenvironment with excess FGF23 [6]. Alternatively, FGF1 might replace FGF23 in this hypothetical autocrine/paracrine loop, as suggested by its high expression levels.

Regarding the mechanism of neoplastic overexpression of FGF23, it is possible that *FN1-FGFR1* fusion might preferentially occur in cells that normally express FGF23, eg osteocytes and their precursors. However, many PMTs occur in the soft tissues, where osteocytes are not normally found, and the quantity of FGF23 expressed by PMT far exceeds physiological levels. This suggests that high-level FGF23 expression might be the result of activated *FN1-FGFR1*, as *FGFR1* signalling has been implicated in FGF23 regulation [7,17]. Our hypothesized autocrine/paracrine model of oncogenic mechanism also suggests that this fusion event might confer evolutionary advantages to subclones of tumour cells that express higher FGF23 levels. The proposed hypotheses of PMT tumorigenesis driven by *FN1-FGFR1* fusion are illustrated in Figure 3B.

Importantly, our findings may have therapeutic implications, as emerging *FGFR1* antagonists have shown some anti-tumour efficacy in clinical trials [18], and might thus have a role in treating malignant and/or inoperable PMT. Moreover, a recent clinical trial has shown some utility of an anti-FGF23 antibody in managing FGF23-induced hypophosphataemic disease [19]. If the binding of FGF23 to *FN1-FGFR1* chimeric proteins should prove critical in PMT oncogenesis, this would additionally support the use of anti-FGF23 antibodies as both symptom-relieving and anti-tumour therapy in PMT.

In conclusion, we have identified a novel *FN1-FGFR1* fusion gene in a significant subset of PMTs.

The chimeric protein might possibly have not only great biological relevance, in terms of both tumourigenesis (via an autocrine/paracrine mechanism) and phenotypes (of FGF23 secretion and the consequent TIO), but also promising therapeutic implications, although verification of these hypotheses requires further study.

## Acknowledgments

This work was supported by grants NTUH 103-N01 from the Department of Medical Research, National Taiwan University Hospital (to J-C Lee) and MOHW103-TD-B-111-04 from the Ministry of Health and Welfare (Taiwan) (to S-H Yang). We thank the NTUH sequencing core laboratory, the NTU Center of Genomic Medicine, and the National Center of Genome Medicine for technical assistance.

## Author contribution statement

J-CL conceived, designed, and implemented this study and wrote the paper. Y-MJ conceived the study and provided technical guidance. S-YS, C-YL, and S-HC performed the bioinformatics analysis and generated figures. C-TW guided the pathological interpretation. K-ST, J-WH, and S-RS provided clinical and laboratory information. C-HL and AM-E provided cases and conceptual input. JMC assisted in obtaining the cases and the clinicopathological data. C-CC implemented experiments and provided conceptual input. ALF provided most of the specimens and authoritative conceptual guidance of PMTs. Y-LC provided strategic supervision. C-WL provided critical resources and interpreted the experimental results.

## References

1. Folpe AL. Phosphaturic mesenchymal tumour. In *World Health Organization Classification of Tumours of Soft Tissue and Bone*, Fletcher CDM, Bridge JA, Hogendoorn PCW, et al (eds). Lyon: IARC Press, 2013; 2.
2. Folpe AL, Fanburg-Smith JC, Billings SD, et al. Most osteomalacia-associated mesenchymal tumors are a single histopathologic entity: an analysis of 32 cases and a comprehensive review of the literature. *Am J Surg Pathol* 2004; 28: 1–30.
3. Shimada T, Mizutani S, Muto T, et al. Cloning and characterization of FGF23 as a causative factor of tumor-induced osteomalacia. *Proc Natl Acad Sci U S A* 2001; 98: 6500–6505.
4. Weidner N, Santa Cruz D. Phosphaturic mesenchymal tumors. A polymorphous group causing osteomalacia or rickets. *Cancer* 1987; 59: 1442–1454.
5. White KE, Larsson TE, Econs MJ. The roles of specific genes implicated as circulating factors involved in normal and disordered phosphate homeostasis: frizzled related protein-4, matrix extracellular phosphoglycoprotein, and fibroblast growth factor 23. *Endocrine Rev* 2006; 27: 221–241.
6. Faul C, Amaral AP, Oskouei B, et al. FGF23 induces left ventricular hypertrophy. *J Clin Invest* 2011; 121: 4393–4408.

7. White KE, Cabral JM, Davis SI, *et al.* Mutations that cause osteogenic dysplasia define novel roles for FGFR1 in bone elongation. *Am J Hum Genet* 2005; **76**: 361–367.
8. Parker BC, Engels M, Annala M, *et al.* Emergence of FGFR family gene fusions as therapeutic targets in a wide spectrum of solid tumours. *J Pathol* 2014; **232**: 4–15.
9. Urakawa I, Yamazaki Y, Shimada T, *et al.* Klotho converts canonical FGF receptor into a specific receptor for FGF23. *Nature* 2006; **444**: 770–774.
10. Jackson CC, Medeiros LJ, Miranda RN. 8p11 myeloproliferative syndrome: a review. *Hum Pathol* 2010; **41**: 461–476.
11. Carter JM, Caron BL, Dogan A, *et al.* A novel chromogenic *in situ* hybridization assay for *FGF23* mRNA in phosphaturic mesenchymal tumors. *Am J Surg Pathol* 2014; DOI: 10.1097/PAS.0000000000000290 (in press).
12. Bonin G, Scamps C, Turc-Carel C, *et al.* Chimeric EWS-FLI1 transcript in a Ewing cell line with a complex t(11;22;14) translocation. *Cancer Res* 1993; **53**: 3655–3657.
13. Liao JY, Lee JC, Wu CT, *et al.* Dedifferentiated liposarcoma with homologous lipoblastic differentiation: expanding the spectrum to include low-grade tumours. *Histopathology* 2013; **62**: 702–710.
14. Graham RP, Hodge JC, Folpe AL, *et al.* A cytogenetic analysis of 2 cases of phosphaturic mesenchymal tumor of mixed connective tissue type. *Hum Pathol* 2012; **43**: 1334–1338.
15. Ren H, Tan ZP, Zhu X, *et al.* Identification of anaplastic lymphoma kinase as a potential therapeutic target in ovarian cancer. *Cancer Res* 2012; **72**: 3312–3323.
16. Shi E, Kan M, Xu J, *et al.* Control of fibroblast growth factor receptor kinase signal transduction by heterodimerization of combinatorial splice variants. *Mol cell Biol* 1993; **13**: 3907–3918.
17. Martin A, Liu S, David V, *et al.* Bone proteins PHEX and DMP1 regulate fibroblastic growth factor Fgf23 expression in osteocytes through a common pathway involving FGF receptor (FGFR) signaling. *FASEB J* 2011; **25**: 2551–2562.
18. Liang G, Chen G, Wei X, *et al.* Small molecule inhibition of fibroblast growth factor receptors in cancer. *Cytokine Growth Factor Rev* 2013; **24**: 467–475.
19. Fukumoto S. Anti-fibroblast growth factor 23 antibody therapy. *Curr Opin Nephrol Hypertens* 2014; **23**: 346–351.
20. Singh P, Carraher C, Schwarzbauer JE. Assembly of fibronectin extracellular matrix. *Annu Rev Cell Dev Biol* 2010; **26**: 397–419.
21. Trapnell C, Pachter L, Salzberg SL. TopHat: discovering splice junctions with RNA-Seq. *Bioinformatics* 2009; **25**: 1105–1111.
22. Edgren H, Murumagi A, Kangaspeka S, *et al.* Identification of fusion genes in breast cancer by paired-end RNA-sequencing. *Genome Biol* 2011; **12**: R6.
23. Anders S, McCarthy DJ, Chen Y, *et al.* Count-based differential expression analysis of RNA sequencing data using R and Bioconductor. *Nature Protoc* 2013; **8**: 1765–1786.

### SUPPORTING INFORMATION ON THE INTERNET

The following supporting information may be found in the online version of this article:

**Supplementary methods.** Details of RNA sequencing data analysis.

**Table S1.** List of the samples of which the RNA sequencing data were compared.

**Table S2.** Sequences of primers used in DNA PCR and RT-PCR.

**Table S3.** Fusion detection in PMTs (fusion point location and spanning read number).

**Table S4.** PMT gene expression (FPKM values) and ranking by RNA sequencing.

**Figure S1.** Heatmap plot on the 31 genes of four PMTs and 28 tumours of other types.

**Figure S2.** EdgeR MDS plot and DeSeq PCA plot of the 30 tumour samples.

**Figure S3.** RT-PCR and PCR confirmation of the genetic fusion.

**Figure S4.** Illustration of chromosomal rearrangement in PMT.